ISSN 2304-3415, Russian Open Medical Journal
2023. Volume 12. Issue 2 (June). Article CID e0206
DOI: 10.15275/rusomj.2023.0206

Original article

Left ventricular segmental strain based on speckle tracking echocardiography versus indications of immune inflammation in patients after COVID-19 pneumonia

Nikita E. Shirokov, Elena I. Yaroslavskaya, Dmitry V. Krinochkin, Nadezhda A. Osokina, Natalia A. Musikhina, Tatyana I. Petelina

Tyumen Cardiology Research Center, Tomsk National Medical Research Center of the Russian Academy of Sciences, Tyumen, Russia

Received 26 September 2022, Revised 30 December 2022, Accepted 28 March 2023

Abstract: *Background* — The significance of cytokine activation and immune inflammation in subclinical damage to cardiomyocytes and resulting development of the congestive heart failure (CHF) is frequently discussed in published studies, as well as whether there are cardiac lesions in COVID-19 survivors identified by the speckle tracking echocardiography (STE).
Objective — To examine the association of echocardiographic parameters with indications of immune inflammation in patients recovered from COVID-19 pneumonia depending on segmental longitudinal strain (LS) of the left ventricle (LV) identified by STE.
Methods — Our study encompassed 216 patients (51.1% men, mean age of 50.1±11.1 years) distributed among two groups: Group I (n=108) included study subjects with segmental LS (≥3 LV segments) revealed by the STE; Group II (n=108) comprised patients without visually detectable LV lesions. All patients were examined three months after COVID-19 pneumonia.
Results — Groups did not differ statistically significantly in terms of LV ejection fraction (68.7±4.3% in Group I vs. 68.6±4.3% in Group II; p=0.916). Global LS was significantly lower in the Group I than in the Group II at the time of the control follow-up visit three months later (-18.2 [-16.7; -19.4] % vs. -20.6 [-19.5; -22.1] %, respectively; p<0.001). When analyzing laboratory indications of immune inflammation in groups, we revealed statistically significantly higher values in Group I vs. Group II in the concentrations of interleukin 6 (3.1 [2.4;3.9] pg/mL vs. 2.5 [3.8;4.7] pg/mL; p=0.009), C-reactive protein (4.7 [2.9;8.3] mg/L vs. 3.0 [1.5; 5.3] mg/L; p<0.001), and tumor necrosis factor α (6.0 [4.8;4.1] pg/ml vs. 5.0 [4.0;6.4] pg/ml; p=0.001). In Group I, we detected diffuse lesion of LS (≥4 segments of the same LV level; 38.0% of patients) and regional lesion of LS (≥3 segments corresponding to the blood supply pools of the anterior, circumflex, or right coronary arteries; 62.0% of patients). According to logistic regression, the LS of the basal LV level (OR 3.028; 95% CI 1.909-4.802; p<0.001) in combination with LS of the apical LV level (OR 1.287; 95% CI 1.099-1.507; p=0.002) and LV lateral wall annular velocity assessed by tissue Doppler imaging, peak e' (OR 0.774; 95% CI 0.657-0.911; p=0.002) had an independent relationship with each of diffuse and regional LS lesions.
Conclusion — Based on STE data, we have identified a relationship of diffuse and regional LV lesions with features of systolic and diastolic LV dysfunction and markers of immune inflammation in patients three months after COVID-19 pneumonia.

Keywords: COVID-19, longitudinal strain, immune inflammation, chronic inflammatory cardiomyopathy, microvascular thrombosis.

Cite as Shirokov NE, Yaroslavskaya EI, Krinochkin DV, Osokina NA, Musikhina NA, Petelina TI. Left ventricular segmental strain based on speckle tracking echocardiography versus indications of immune inflammation in patients after COVID-19 pneumonia. *Russian Open Medical Journal* 2023; 12: e0206.

Correspondence to Nikita Shirokov. Phone: +79829453854. E-mail: shirokov.ne@mail.ru.

Introduction

SARS-CoV-2 induces a massive release of proinflammatory cytokines in COVID-19-associated macrophage activation syndrome resulting in microvascular thrombosis in the pulmonary arterial network [1]. It is essential to know whether the immunothrombotic response underlies the long-term consequences of COVID-19 [2,3]. Long-term excessive release of proinflammatory cytokines leads to endothelial dysfunction, damage to cardiomyocytes (CMC), and collagen accumulation with subsequent myocardial remodeling and congestive heart failure (CHF) [4].

Myocardial damage in COVID-19 was confirmed by Lindner D. et al. during autopsy: virus particles were found in the heart tissue of 61.5% of patients [5]. In 30-50% of patients, three months after COVID-19, myocarditis-like accumulation of gadolinium was detected by MRI in the middle and subepicardial layers of the left ventricular (LV) myocardium [6,7]. Speckle tracking echocardiography (STE) revealed a predominantly subepicardial (rather than subendocardial) decrease in LV contractility [8,9].

It is worth noting that STE method, according to Shah S.J. et al., can serve as a digital biopsy capable of evaluating the function of CMC [10]. At the same time, various authors reported the lesions of LS based on STE data, with various options for the predominant localization of the lesion [11,12].

Objective: To examine the association between echocardiographic parameters and laboratory indicators of immune inflammation in patients recovered from COVID-19

pneumonia depending on segmental longitudinal strain of the left ventricle identified by the speckle tracking echocardiography.

Material and methods

Subjects

Ethical approval: All procedures performed in studies involving human participants were in accordance with the ethical standards of the institutional and/or national research committee and with the 1964 Declaration of Helsinki and its later amendments or comparable ethical standards.

Our study was enumerated in the international register of clinical trials of the USA National Institute of Health (ClinicalTrials.gov Identifier: NCT04501822). The study protocol was approved by the local ethics committee (No.159 of 23 July 2020). Informed consent was obtained from every patient included in the study.

The inclusion criteria for our study were: pneumonia associated with COVID-19 officially diagnosed at the regional clinical hospital and the patient's willingness to participate in outpatient monitoring. The exclusion criteria were as follows: chronic diseases in the acute stage, tuberculosis and other diseases accompanied by pulmonary fibrosis, valvular heart disease, cancer, HIV, and chronic hepatitis.

Patients who experienced COVID-19 pneumonia were examined three months after two consecutive negative results of polymerase chain reaction test. STE method with high quality of imaging was applied to 273 of 380 patients (71.8%) included in the *Prospective Register of Survivors of Pneumonia Associated with COVID-19* (certificate of state registration No. 2021622535). Subsequently, patients with confirmed coronary artery disease (CAD) [13], arterial hypertension (AH) and increased LV myocardial mass were excluded [14]. Consequently, the study involved 216 patients (56.8%) (51.1% men, mean age of 50.1±11.1 years).

Analyzing echocardiography

Echocardiography was performed using the expert-class ultrasound system Vivid S70 and matrix sensor M5Sc-D (1.5-4.6 MHz); the data were saved in the DICOM format. Myocardial LS was assessed by STE in accordance with the current recommendations [15] using the 17-segment LV model to visually assess the nature of its lesion (*Figure* 1). Patients with a lesion of segmental LS (≥3 LV segments) constituted Group I (n=108); study subjects without LS impairment formed Group II (n=108) [16]. Lesions of ≥4 segments of the same LV level were considered diffuse LS impairment (*Figure* 1). A decrease in LS ≥3 segments corresponding to the blood supply basins of the anterior, circumflex, or right coronary arteries were considered a regional lesion of the left ventricle (*Figure* 2).

Laboratory data

Laboratory studies included a complete blood count and blood biochemistry test. We determined the biochemical markers of inflammation. High-sensitivity C-reactive protein (hsCRP, reference value range: 0-3.0 mg/L) was identified by immunoturbidimetric method with the *C-reactive protein hs analytical kit* (BioSystem, Spain) on a semi-automatic analyzer of the open type (Clima MC-15, Spain). Interleukin (IL) 6 (IL-6, reference value range of ≥9.7 pg/mL), IL-1 (reference value range of 0-5 pg/mL), IL-8 (reference value range of 0-62 pg/mL), tumor necrosis factor α (TNF-α, reference value range of 0-8.11 pg/mL), homocysteine (reference value range of 5.0-15.0 μmol/L), and N-terminal pro-brain natriuretic peptide (NT-proBNP) were measured by competitive method (solid-phase chemiluminescent enzyme immunoassay) on the IMMULITE 2000 analyzer (Siemens Diagnostics, USA).

Figure 1. Diffuse lesion of predominantly basal level of the LV (LS at the basal level =15.3%; LS at the mid-ventricular level =17.6%; LS at the apical level =17.8%; GLS =16.5%).

LV, left ventricle; LS, longitudinal strain; GLS, global longitudinal strain.

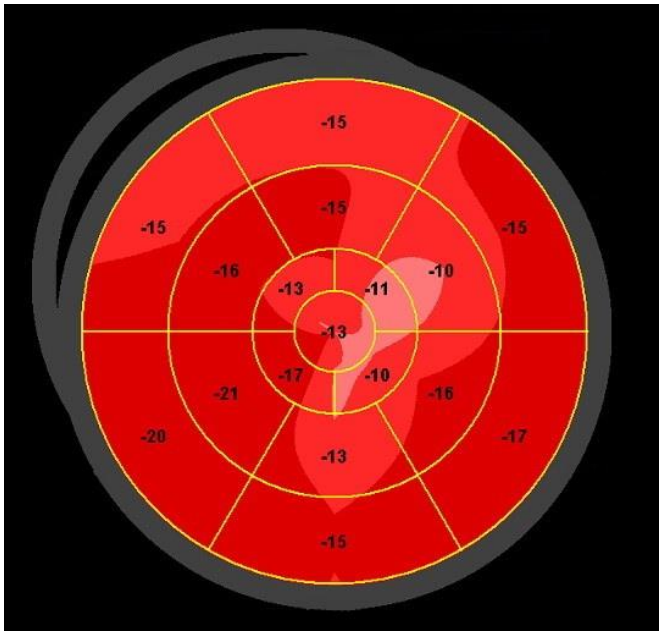

Figure 2. Regional lesion of the apical anterior and apical septal segments of the LV (LS at the basal level =16.2%; LS at the mid-ventricular level =15.2%; LS at the apical level =12.8%; GLS =15.5%)

LV, left ventricle; LS, longitudinal strain; GLS, global longitudinal strain.

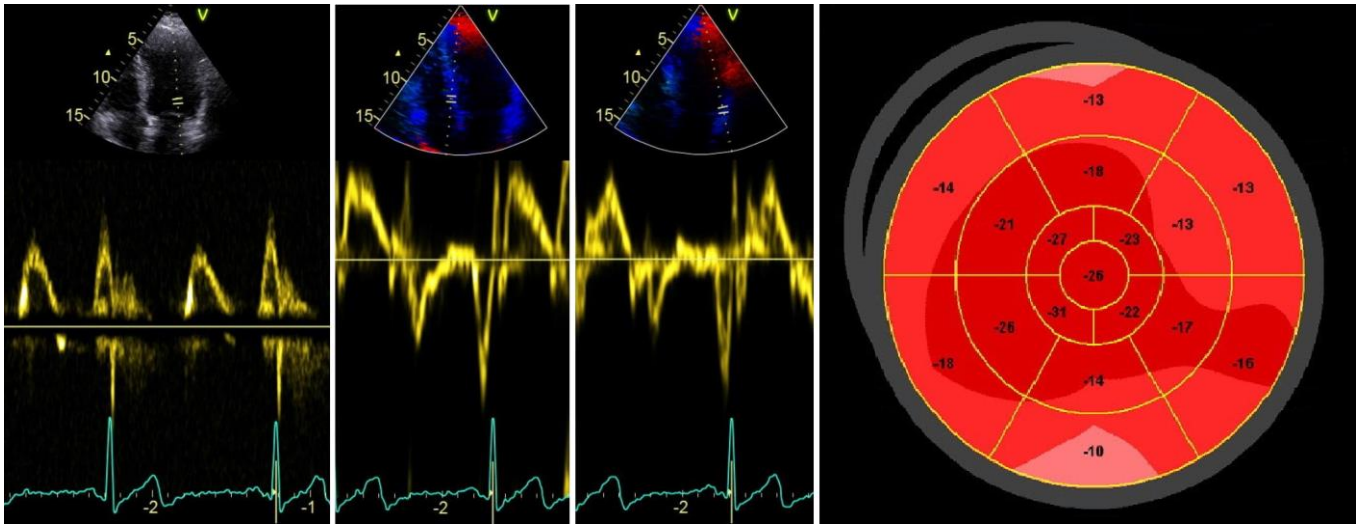

Figure 3. A patient with symptoms of diastolic dysfunction (transmitral flow: peak E=57 cm/s, peak A=86 cm/s; TDI e': IVS=9 cm/s and lateral wall of the LV=8 cm/s) and impaired contractility of the LV (LS at the basal level =14.0%; preservation of the GLS=19.2%; LS at the apical segments =25.8%).

GLS, global longitudinal strain; IVS, interventricular septum; LV, left ventrile; TDI, tissue Doppler imaging.

Table 1. Clinical characteristics of patients three months after COVID-19 pneumonia

Indicator	*Group I (n=108)*	*Group II (n=108)*	*p*
Age, years	51.3±10.9	48.8±11.2	0.109
Gender, male, %	64.8	36.1	<0.001
BMI, kg/m^2	30.1 [27.8;33.8]	27.5 [24.3;31.2]	<0.001
AH, %	79.6	54.6	<0.001
DM, %	9.3	5.6	0.437
HFA-PEFF diagnostic algorithm score ≥2, %	47.2	26.9	0.003
Pneumonia on CT during hospitalization, %	51.6±20.4	47.8±19.9	0.199
Pneumonia on CT at the control point, %	14.5 [7.0;31.8]	8.0 [5.0;24.0]	0.328
Dyspnea, %	28.7	31.5	0.767
Weakness, %	43.5	46.3	0.784
Fatigue, %	41.7	48.7	0.412
Chest pain, %	23.1	26.9	0.638
All symptoms, %	61.6	59.3	0.890

BMI, body mass index; AH, arterial hypertension; DM, diabetes mellitus; FC, functional class; CHF, congestive heart failure; NYHA, New York Heart Association; CT, computed tomography; HFA-PEFF, The Heart Failure Association preserved ejection fraction.

Table 2. Characterization of conventional echocardiographic parameters in patients three months after COVID-19 pneumonia

Parameter	*Group I (n=108)*	*Group II (n=108)*	*p*
LV EF, %	68.7±4.3	68.6±4.3	0.916
LV EDV, ml	95.0 [77.0;110.0]	81.5 [68.0;100.8]	0.003
LA EDV, ml	47.3±13.6	45.2±11.9	0.230
IVS thickness, mm	10.0 [10.0;11.8]	10.0 [9.0;10.8]	<0.001
LV posterior wall thickness, mm	10.0 [9.0;10.0]	9.0 [9.0;10.0]	<0.001
LV myocardial mass index, g/m^2	79.0 [67.8;86.6]	69.0 [60.9;80.3]	0.001
Peak E, transmitral flow, cm/s	66.0 [57.0;75.5]	75.0 [64.0;89.0]	<0.001
Peak A, transmitral flow, cm/s	71.1±16.8	67.8±18.3	0.164
DT, transmitral flow, ms	219.8±63.8	206.3±57.1	0.109
TDI e', IVS, cm/s	7.0 [6.0;9.0]	9.0 [8.0;12.0]	<0.001
TDI e', LV lateral wall, cm/s	9.0 [8.0;12.0]	12.0 [10.0;15.0]	<0.001
Peak S, PV, cm/s	57.3±9.7	59.8±11.0	0.087
Peak D, PV, cm/s	40.0±9.4	42.8±10.8	0.043
Peak Ar, PV, cm/s	32.9±7.0	32.5±7.1	0.697

LV, left ventricular; EF, ejection fraction; EDV, end diastolic volume; LA, left atrial; IVS, interventricular septum; DT, deceleration time (peak E of transmitral flow); TDI e', left ventricular annular velocity assessed by tissue Doppler imaging, peak e'; PV, pulmonary veins.

Table 3. LV longitudinal strain in patients three months after COVID-19 pneumonia

Indicator	*Group I (n=108)*	*Group II (n=108)*	*p*
1, %	-16.0 [-12.0; -18.0]	-18.0 [-17.0; -21.0]	<0.001
2, %	-16.0 [-13.0; -18.0]	-18.0 [-16.0; -20.0]	<0.001
3, %	-16.0 [-14.0; -17.8]	-18.0 [-16.0; -19.0]	<0.001
4, %	-18.0 [-16.0; -21.0]	-20.0 [-19.0; -22.0]	<0.001
5, %	-16.0 [-14.0; -19.0]	-20.0 [-17.3; -22.0]	<0.001
6, %	-16.0 [-13.0; -18.0]	-19.0 [-17.0; -21.0]	<0.001
7, %	-16.0 [-13.0; -19.0]	-19.0 [-17.0; -22.0]	<0.001
8, %	-19.0 [-17.0; -22.0]	-21.0 [-19.0; -23.0]	<0.001
9, %	-20.0 [-18.0; -21.0]	-21.0 [-20.0; -23.0]	<0.001
10, %	-20.0 [-18.0; -22.8]	-22.0 [-20.0; -24.0]	<0.001
11, %	-18.0 [-15.0; -19.0]	-21.0 [-19.0; -23.0]	<0.001
12, %	-16.0 [-14.0; -18.0]	- 20.0[-17.0; -22.0]	<0.001
13, %	-19.8±5.3	-22.0±4.9	0.002
14, %	-23.0 [-20.0; -26.0]	-25.0 [-22.0; -27.0]	<0.001
15, %	-21.5 [-19.0; -25.0]	-24.0 [-22.0; -27.0]	<0.001
16, %	-19.0 [-16.0; -22.0]	-23.0 [-19.3; -25.0]	<0.001
17, %	-21.0 [-18.0; -24.0]	- 23.0[-21.0; -26.0]	<0.001
Basal level, %	-16.2 [-15.3; -17.2]	-18.9 [-18.0; -20.0]	<0.001
Mid-ventricular level, %	-17.8 [-17.0; -19.2]	-20.6 [-19.5; -22.0]	<0.001
Apical level, %	-20.6 [-17.9; -24.0]	-23.3 [-20.5; -26.0]	<0.001
GLS, %	-18.2 [-16.7; -19.4]	-20.6 [-19.5; -22.1]	<0.001
Reduced GLS <-18.0%, %	42.6	4.6	<0.001
Number of visually damaged LV segments, n	5.0 [4.0; 6.8]	1.0 [0.0; 2.0]	<0.001

Segmental longitudinal strain (sensu the guidelines for echocardiography cardiac segmentation model in adults [14]: 1 – basal anterior segment; 2 – basal anteroseptal segment; 3 – basal inferoseptal segment; 4 – basal inferior segment; 5 – basal inferolateral segment; 6 – basal anterolateral segment; 7 – mid anterior segment; 8 – mid anteroseptal segment; 9 – mid inferoseptal segment; 10 – mid inferior segment; 11 – mid inferolateral segment; 12 – mid anterolateral segment; 13 – apical anterior segment; 14 – apical septal segment; 15 – apical inferior segment; 16 – apical lateral segment; 17 – apex. GLS, global longitudinal strain; LV, left ventricle.

Statistical data processing

Statistical data processing was carried out using the Statistical Package for the Social Sciences – IBM SPSS Statistics 26. The normality of distributions was checked by the Kolmogorov-Smirnov criterion. Pearson's χ2 test was applied to compare qualitative variables. We employed Student's t-test to compare the quantitative variables in case of their normal distribution; the results are presented as M±SD (M: mean; SD: standard deviation). When analyzing quantitative variables with a distribution other than normal, the Mann-Whitney U test was used; results are presented as median with an interquartile range of the 25th and 75th percentiles. Spearman's rank-order correlation analysis was carried out to determine the severity of relationships. Logistic regression analysis was used to identify an independent relationship. When assessing the diagnostic significance of the indicators obtained in the regression, ROC analysis was employed. The statistical significance of differences in variables was assumed at $p < 0.05$.

Results

Clinical, functional and laboratory characteristics of patients are presented in *Tables* 1-4.

The groups were comparable in terms of the main clinical and functional characteristics three months after COVID-19 pneumonia, with the exception of gender, AH, and body mass index (BMI), which were statistically significantly more common in Group I. There were no significant differences in the severity of lung damage based on the chest computed tomography during hospitalization and at the control point. The groups were also comparable in terms of post COVID-19 syndrome symptoms. However, the scores of the diagnostic algorithm, *The Heart Failure Association preserved ejection fraction* (HFA-PEFF), were significantly higher in Group I, compared with Group II (*Table* 1).

LV end diastolic volume and LV myocardial mass index had statistically significantly higher values in Group I patients vs. Group II. There was also a significant reduction in the early diastolic annular velocity according to tissue Doppler imaging (TDI), along with the early diastolic velocity of the transmitral flow and diastolic flow velocity in the pulmonary veins according to pulsed wave Doppler in Group I, as compared to Group II (*Table 2*, *Figure* 3).

Analysis of LV contractile function yielded no significant differences in LV ejection fraction, but detected lesions of both GLS (global longitudinal strain) and LS of all LV levels in Group I, compared with Group II (*Tables 2*,3). Analysis of the segmental LS revealed impairment of contractility of most LV segments in Group I (*Table* 3). Among Group I patients, we discovered diffuse lesion of LS (n=41, 38.0% of patients) and regional lesion of LV (n=67, 62.0% of patients).

Table 4. Laboratory indicators in patients three months after COVID-19 pneumonia

Indicator	*Group I (n=108)*	*Group II (n=108)*	*p*
Red blood cells, $\times 10^{12}$/L	5.0 [4.8;5.3]	4.7 [4.5;5.1]	<0.001
Hemoglobin, g/L	146.0 [136.0;152.3]	136.0 [128.0;145.3]	<0.001
Ferritin, μg/L	99.1 [43.5;148.9]	51.0[23.2;158.9]	0.068
White blood cells, $\times 10^{9}$/L	5.3±1.6	5.2±1.4	0.186
Neutrophils, %	53.5±8.8	54.9±8.3	0.244
Lymphocytes, %	36.4±8.2	35.1±7.5	0.247
Eosinophils, %	2.5±1.8	2.6±1.7	0.550
Platelets, $\times 10^{9}$/l	233.1±51.6	236.8±63.5	0.645
CPK, u/L	118.9±62.9	120.2±81.1	0.895
CK-MB, u/L	12.4±5.2	13.1±5.6	0.349
AST, u/L	20.9 [16.2;27.0]	20.0 [15.9;23.8]	0.063
ALT, u/L	23.0 [16.4;32.3]	21.2 [15.9;26.6]	0.036
Creatinine, μg/L	76.3 [68.9;85.5]	69.6 [61.6;78.1]	<0.001
GFR, mg/mmol	91.7±16.1	92.2±14.8	0.837
Glucose, mmol/l	5.5±1.0	5.4±0.7	0.449
Fibrinogen, g/L	2.8±0.6	2.6±0.6	0.162
PTR, %	100.9±9.8	99.5±13.4	0.481
TC, mmol/L	5.7±1.2	5.5±1.3	0.473
HDL cholesterol, mmol/L	1.2 [1.0;1.4]	1.3 [1.1;1.7]	0.002
LDL cholesterol, mmol/L	3.5±1.0	3.4±1.2	0.624
VLDL cholesterol, mmol/L	0.7 [0.5;1.0]	0.5 [0.4;0.7]	<0.001
TG, mmol/L	1.4 [1.1;2.2]	1.1 [0.8;1.5]	<0.001
D-dimer, μg/L	0.2 [0.1;0.3]	0.2 [0.1;0.4]	0.353
NT-proBNP, pg/mL	68.8 [30.5;134.0]	63.1 [15.1;146.0]	0.390
hsCRP, mg/L	4.7 [2.9;8.3]	3.0 [1.5;5.3]	<0.001
TNF-α, pg/mL	6.0 [4.8;7.1]	5.0 [4.0;6.4]	0.001
Homocysteine, μmol/l	13.1±4.7	12.8±5.3	0.584
IL-1, pg/mL	2.2±1.0	2.2±1.0	0.918
IL-6, pg/mL	3.1 [2.4;3.9]	2.5[3.8;4.7]	0.009
IL-8, pg/mL	15.4±8.6	15.1±8.0	0.786

CPK, creatine phosphokinase; CK-MB, creatine kinase MB isoenzyme; AST, aspartate aminotransferase; ALT, alanine transaminase; GFR, glomerular filtration rate; PTR, prothrombin ratio; TC, total cholesterol; HDL, high-density lipoproteins; LDL, low-density lipoproteins; VLDL, very-low-density lipoproteins; TG, triglycerides; NT-proBNP, N-terminal pro-brain natriuretic peptide; hsCRP, high-sensitivity C-reactive protein; TNF-α, tumor necrosis factor α; IL, interleukin.

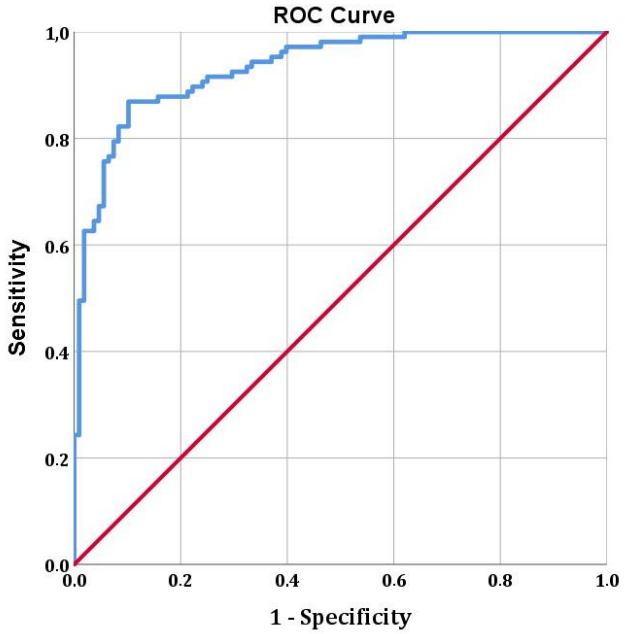

Figure 4. Sensitivity and specificity of the independent association of the baseline complex of variables with diffuse and regional LS lesions.
LS, longitudinal strain.

Analysis of the laboratory indicators yielded statistically significantly higher concentrations of TNF–α, IL-6, triglycerides, hsCRP and some other indicators in Group I vs. Group II (*Table 4*).

In Group II, based on Spearman's correlation analysis, we revealed weak correlations between the concentration of ferritin and LS at the basal LV level (r=-0.250, p=0.033), the concentration of ferritin and LS at the mid-ventricular level of the LV (r=-0.262, p=0.025), the concentration of hsCRP and LS at the mid-ventricular level of the LV (r=-0.197, p=0.043), and the concentration of CRP and LS at the apical level of the LV (r=-0.192, p=0.049).

According to logistic regression data, of all baseline variables describing LV systolic and diastolic functions, laboratory biomarkers, and clinical characteristics, solely the complex of LS at the basal LV level (OR 3.028; 95% CI 1.909-4.802; p<0.001), LS at the apical LV level (OR 1.287; 95% CI 1.099-1.507; p=0.002) and TDI (peak e') of the LV lateral wall (OR 0.774; 95% CI 0.657-0.911; p=0.002) had an independent association with diffuse and regional lesions of LS. In ROC analysis, the sensitivity and specificity of this model were 86.9% and 89.8%, respectively. The area under the curve (AUC) was 0.934 (p<0.001), which corresponded to the excellent quality of the predictive model (*Figure 4*).

Discussion

The COVID-19 pandemic has generated interest in the concept of immunothrombotic response, as the disease is a relevant model for demonstrating the mutually potentiating action of the immune system and the coagulation system [3].

In our study, among patients with LS impairment assessed by STE, diffuse and regional LV lesions were identified. In patients who underwent COVID-19, a predominant lesion at the basal level, along with posterior and lateral walls, of the LV was revealed by STE [11,12], which is consistent with our results (*Figure 1*). Moreover, this localization corresponds to the lesion of the LV in myocarditis according to MRI [7]. On the other hand, microvascular thrombi in coronary arteries and infection of endothelial cells have been confirmed in SARS-CoV-2 [17]. Thus, diffuse and regional LV lesions assessed by STE three months after COVID-19 pneumonia may indicate chronic inflammatory cardiomyopathy and coronary microvascular dysfunction, respectively [18,19] (*Figure 1*, *2*).

It is assumed that the proinflammatory cytokine (IL-6)) makes a significant contribution to immune dysregulation [20]. In the absence of regulation, neutrophil extracellular traps (NETs) can contribute to the intensification of inflammation and microvascular thrombosis. It is important to note that a weak correlation of NETs features with CRP concentration was discovered [21]. At the same time, elevated levels of hsCRP and ferritin were used as pilot prognostic criteria for the cytokine storm associated with COVID-19. Elevated triglyceride levels in these patients were also noted [22]. In addition, a reduction in GLS was associated with high levels of IL-6, hsCRP, and ferritin 30-45 days after COVID-19. Hence, a longer follow-up monitoring duration of patients with latent LV dysfunction was proposed [23].

According to our data, in patients with visually noticeable lesions of the LV based on STE, three months after pneumonia associated with COVID-19, the level of laboratory parameters involved in the implementation of the immune-inflammatory response was higher, but still within the normal range (with the exception of CRP). As is known, hsCRP is synthesized in response to the release of IL-6 and TNF-α [24]. It should also be pointed out that elevated levels of cytokines, TNF-α and IL-6, lead to inadequate CMC contact due to displacement of the desmosomal protein, plakoglobin, from the membrane. This contributes to cell membrane damage and fibrofatty replacement of CMC [25,26]. Therefore, it is important state that we have established a decrease in LS of most LV segments without visual markers of their dysfunction in patients with diffuse and regional LV lesions.

SARS-CoV-2 enters the CMC by binding its own spike protein to the membrane protein of angiotensin-converting enzyme 2 (ACE2) [27]. Moreover, an association was found between the immune response and myocardial inflammation in patients with COVID-19 and overexpression of ACE2 in CMC in CHF [28]. It should be noted that we detected AH and diastolic dysfunction more often in patients with impaired LV contractility. Besides, nearly 60% of patients have post COVID-19 syndrome, which includes shortness of breath and chest pain [29]. In addition, HFA-PEFF diagnostic algorithm scores were higher in patients with impaired LV contractility. Therefore, it seems relevant to suggest that such patients have CHF with preserved LV ejection fraction and to conduct a diastolic stress test [30].

Limitations

First, our sample size, while relatively larger than in previous studies, was still somewhat small and subject to the limitations of small groups. Second, all patients were confirmed to have COVID-19. We did not have follow-up data from patients who have not had COVID-19. Finally, the division into groups used by us was not previously described. Accordingly, we can only speculate on a probably cause for the association between echocardiographic parameters and symptoms of immune inflammation three months after COVID-19 associated pneumonia (chronic inflammatory cardiomyopathy or coronary microvascular dysfunction).

Conclusion

Based on speckle tracking echocardiography data, we have identified a relationship of diffuse and regional lesions of the left ventricle with features of systolic and diastolic dysfunction of the left ventricle and markers of immune inflammation in patients three months after COVID-19 pneumonia.

Conflict of Interest

The authors declare that they have no conflicts of interest regarding the presented article. The authors are accountable for all aspects of the study in terms of ensuring the accuracy and integrity of any part of the research.

Funding

No external funding was provided.

References

1. McGonagle D, O'Donnell JS, Sharif K, Emery P, Bridgewood C. Immune mechanisms of pulmonary intravascular coagulopathy in COVID-19 pneumonia. *Lancet Rheumatol* 2020; 2(7): e437-e445. https://doi.org/10.1016/s2665-9913(20)30121-1.
2. Yelin D, Wirtheim E, Vetter P, Kalil AC, Bruchfeld J, Runold M., et al. Long-term consequences of COVID-19: Research needs. *Lancet Infect Dis* 2020; 20(10): 1115-1117. https://doi.org/10.1016/s1473-3099(20)30701-5.
3. Jayarangaiah A, Kariyanna PT, Chen X, Jayarangaiah A, Kumar A. COVID-19-associated coagulopathy: An exacerbated immunothrombosis response. *Clin Appl Thromb Hemost* 2020; 26: https://doi.org/10.1177/1076029620943293.
4. Van Linthout SV, Tschöpe C. Inflammation – Cause or consequence of heart failure or both? Curr Heart Fail Rep 2017; 14(4): 251-265. https://doi.org/10.1007/s11897-017-0337-9.
5. Lindner D, Fitzek A, Bräuninger H, Aleshcheva G, Edler C, Meissner K. et al. Association of cardiac infection with SARS-CoV-2 in confirmed COVID-19 autopsy cases. *JAMA Cardiol* 2020; 5(11): 1281-1285. https://doi.org/10.1001/jamacardio.2020.3551.
6. Haberka M, Rajewska-Tabor J, Wojtowicz D, Jankowska A, Miszalski-Jamka K, Janus M, et al. Perimyocardial injury specific for SARS-CoV-2-induced myocarditis in comparison with non-COVID-19 myocarditis: A multicenter CMR study. *JACC Cardiovasc Imaging* 2022; 15(4): 705-707. https://doi.org/10.1016/j.jcmg.2021.11.002.
7. Wang H, Li R, Zhou Z, Jiang H, Yan Z, Tao X, et al. Cardiac involvement in COVID-19 patients: Mid-term follow up by cardiovascular magnetic resonance. *J Cardiovasc Magn Reson* 2021; 23(1): 14. https://doi.org/10.1186/s12968-021-00710-x.
8. Li R, Wang H, Ma F, Cui GL, Peng LY, Li CZ, et al. Widespread myocardial dysfunction in COVID-19 patients detected by myocardial strain imaging using 2-D speckle-tracking echocardiography. *Acta Pharmacol Sin* 2021; 42(10): 1567-1574. https://doi.org/10.1038/s41401-020-00595-z.
9. D'Andrea A, Cante L, Palermi S, Carbone A, Ilardi F, Sabatella F, et al. COVID-19 Myocarditis: Prognostic role of bedside speckle-tracking echocardiography and association with total scar burden. *Int J Environ Res Public Health* 2022; 19(10): 5898. https://doi.org/10.3390/ijerph19105898.
10. Shah SJ. 20th Annual Feigenbaum Lecture: Echocardiography for precision medicine – Digital biopsy to deconstruct biology. *J Am Soc Echocardiogr* 2019; 32(11): 1379-1395.e2. https://doi.org/10.1016/j.echo.2019.08.002.
11. Caiado LDC, Azevedo NC, Azevedo RRC, Caiado BR. Cardiac involvement in patients recovered from COVID-19 identified using left ventricular longitudinal strain. *J Echocardiogr* 2021; 20(1): 51-56. https://doi.org/10.1007/s12574-021-00555-4.
12. Tryfou ES, Kostakou PM, Chasikidis CG, Kostopoulos VS, Serafetinidis II, Ferdianaki EK, et al. Biventricular myocardial function in Covid-19 recovered patients assessed by speckle tracking echocardiography: A prospective cohort echocardiography study. *Int J Cardiovasc Imaging* 2021; 38(5): 995-1003. https://doi.org/10.1007/s10554-021-02498-4.
13. Knuuti J, Wijns W, Saraste A, Capodanno D, Barbato E, Funck-Brentano C, et al. ESC Scientific Document Group. 2019 ESC Guidelines for the diagnosis and management of chronic coronary syndromes. *Eur Heart J* 2020; 41(3): 407-477. https://doi.org/10.1093/eurheartj/ehz425.
14. Williams B, Mancia G, Spiering W, Agabiti Rosei E, Azizi M, Burnier M, et al. ESC Scientific Document Group. 2018 ESC/ESH Guidelines for the management of arterial hypertension. *Eur Heart J* 2018; 39(33): 3021-3104. https://doi.org/10.1093/eurheartj/ehy339.
15. Lang RM, Badano LP, Mor-Avi V, Afilalo J, Armstrong A, Ernande L, et al. Recommendations for cardiac chamber quantification by echocardiography in adults: An update from the American Society of Echocardiography and the European Association of Cardiovascular Imaging. *J Am Soc Echocardiogr* 2015; 28(1): 1-39.e14. https://doi.org/10.1016/j.echo.2014.10.003.
16. Benyounes N, Lang S, Gout O, Ancédy Y, Etienney A, Cohen A. Could quantitative longitudinal peak systolic strain help in the detection of left ventricular wall motion abnormalities in our daily echocardiographic practice? *Arch Cardiovasc Dis* 2016; 109(10): 533-541. https://doi.org/10.1016/j.acvd.2016.02.007.
17. Bearse M, Hung YP, Krauson AJ, Bonanno L, Boyraz B, Harris CK, et al. Factors associated with myocardial SARS-CoV-2 infection, myocarditis, and cardiac inflammation in patients with COVID-19. *Mod Pathol* 2021; 34(7): 1345-1357. https://doi.org/10.1038/s41379-021-00790-1.
18. Ammirati E, Frigerio M, Adler ED, Basso C, Birnie DH, Brambatti M, et al. Management of acute myocarditis and chronic inflammatory cardiomyopathy: An expert consensus document. *Circ Heart Fail* 2020; 13(11): e007405. https://doi.org/10.1161/circheartfailure.120.007405.
19. Camici PG, Crea F. Coronary microvascular dysfunction. *N Engl J Med* 2007; 356(8): 830-840. https://doi.org/10.1056/nejmra061889.
20. Moore JB, June CH. Cytokine release syndrome in severe COVID-19. *Science* 2020; 368(6490): 473-474. https://doi.org/10.1126/science.abb8925.
21. Zuo Y, Yalavarthi S, Shi H, Gockman K, Zuo M, Madison JA, et al. Neutrophil extracellular traps in COVID-19. *JCI Insight* 2020; 5(11): e138999. https://doi.org/10.1172/jci.insight.138999.
22. Caricchio R, Gallucci M, Dass C, Zhang X, Gallucci S, Fleece D, et al. Preliminary predictive criteria for COVID-19 cytokine storm. *Ann Rheum Dis* 2021; 80(1): 88-95. https://doi.org/10.1136/annrheumdis-2020-218323.
23. Mahajan S, Kunal S, Shah B, Garg S, Palleda GM, Bansal A, et al. Left ventricular global longitudinal strain in COVID-19 recovered patients. *Echocardiography* 2021; 38(10): 1722-1730. https://doi.org/10.1111/echo.15199.
24. Ridker PM. C-reactive protein: Eighty years from discovery to emergence as a major risk marker for cardiovascular disease. *Clin Chem* 2009; 55(2): 209-215. https://doi.org/10.1373/clinchem.2008.119214.
25. Asimaki A, Tandri H, Duffy ER, Winterfield JR, Mackey-Bojack S, Picken MM, et al Altered desmosomal proteins in granulomatous myocarditis and potential pathogenic links to arrhythmogenic right ventricular cardiomyopathy. *Circ Arrhythm Electrophysiol* 2011; 4(5): 743-752. https://doi.org/10.1161/circep.111.964890.
26. Campian ME, Verberne HJ, Hardziyenka M, de Groot EA, van Moerkerken AF, van Eck-Smit BL, et al. Assessment of inflammation in patients with arrhythmogenic right ventricular cardiomyopathy/dysplasia. *Eur J Nucl Med Mol Imaging* 2010; 37(11): 2079-2085. https://doi.org/10.1007/s00259-010-1525-y.
27. Hoffmann M, Kleine-Weber H, Schroeder S, Krüger N, Herrler T, Erichsen S, et al. SARS-CoV-2 cell entry depends on ACE2 and TMPRSS2

and is blocked by a clinically proven protease inhibitor. *Cell* 2020; 181(2): 271-280. https://doi.org/10.1016/j.cell.2020.02.052.

28. Guo J, Wei X, Li Q, Li, L, Yang, Z, Shi Y, et al. Single-cell RNA analysis on ACE2 expression provides insights into SARS-CoV-2 potential entry into the bloodstream and heart injury. *J Cell Physiol* 2020; 235(12): 9884-9894. https://doi.org/10.1002/jcp.29802.
29. Yong SJ. Long COVID or post-COVID-19 syndrome: Putative pathophysiology, risk factors, and treatments. *Infect Dis (Lond)* 2021; 53(10): 737-754. https://doi.org/10.1080/23744235.2021.1924397.
30. Ha JW, Andersen OS, Smiseth OA. Diastolic stress test: Invasive and noninvasive testing. *JACC Cardiovasc Imaging* 2020; 13(1 Pt 2): 272-282. https://doi.org/10.1016/j.jcmg.2019.01.037.

Authors:
Nikita E. Shirokov – MD, PhD, Researcher, Laboratory of Instrumental Diagnostics, Division of Instrumental Research Methods, Tyumen Cardiology Research Center, Tomsk National Medical Research Center of the Russian Academy of Sciences, Tyumen, Russia. https://orcid.org/0000-0002-4325-2633.
Elena I. Yaroslavskaya – MD, PhD, Professor, Department of Educational Methodology, Head of the Laboratory of Instrumental Diagnostics, Division of Instrumental Research Methods, Tyumen Cardiology Research Center, Tomsk National Medical Research Center of the Russian Academy of Sciences, Tyumen, Russia. https://orcid.org/0000-0003-1436-8853.
Dmitry V. Krinochkin – MD, PhD, Head of the Department of Ultrasound Diagnostics, Senior Researcher, Laboratory of Instrumental Diagnostics, Division of Instrumental Research Methods, Tyumen Cardiology Research Center, Tomsk National Medical Research Center of the Russian Academy of Sciences, Tyumen, Russia. https://orcid.org/0000-0003-4993-056X.
Nadezhda A. Osokina – Laboratory Assistant, Laboratory of Instrumental Diagnostics, Division of Instrumental Research Methods, Tyumen Cardiology Research Center, Tomsk National Medical Research Center of the Russian Academy of Sciences, Tyumen, Russia. https://orcid.org/0000-0002-3928-8238.
Natalia A. Musikhina – MD, PhD, Head of the Department of Emergency Cardiac Care, Division of Clinical Cardiology, Tyumen Cardiology Research Center, Tomsk National Medical Research Center of the Russian Academy of Sciences, Tyumen, Russia. https://orcid.org/0000-0002-8280-2028.
Tatyana I. Petelina – MD, PhD, Deputy Director for Research, Professor, Department of Educational Methodology, Head of the Laboratory of Clinical Diagnostics and Molecular Genetics Studies, Tyumen Cardiology Research Center, Tomsk National Medical Research Center of the Russian Academy of Sciences, Tyumen, Russia. https://orcid.org/0000-0001-6251-4179.